ACS OMEGA

http://pubs.acs.org/journal/acsodf

Article

Novel Anionic–Nonionic Surfactant Based on Water–Solid Interfacial Wettability Control for Residual Oil Development

Lin Li,* Yue Sun, Xiao Jin, Zizhao Wang, Yunbo Dong, Caili Dai, Mingwei Zhao, and Yining Wu

Cite This: *ACS Omega* 2023, 8, 21341−21350

Read Online

ACCESS | Metrics & More | Article Recommendations | Supporting Information

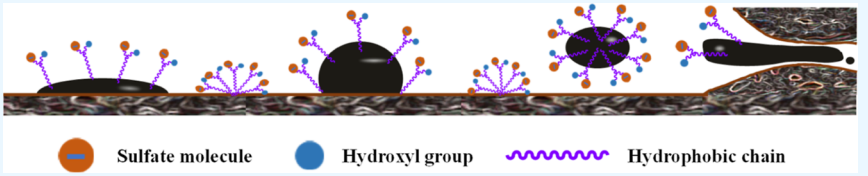

ABSTRACT: Irreversible colloidal asphaltene adsorption layers are formed on formation rock surfaces due to long-term contact with crude oil, and large amounts of crude oil adhere to these oil−wet layers to form residual oil films. This oil film is difficult to peel off due to the strong oil−solid interface effect, which seriously restricts further improvement in oil recovery. In this paper, the novel anionic−nonionic surfactant sodium laurate ethanolamide sulfonate (HLDEA) exhibiting strong wetting control was synthesized by introducing sulfonic acid groups into the nonionic surfactant laurate diethanolamide (LDEA) molecule through the Williamson etherification reaction. The introduction of the sulfonic acid groups greatly improved the salt tolerance and the absolute value of the zeta potential of the sand particles. The experimental results showed that HLDEA altered the wettability of the rock surface from oleophilic to strongly hydrophilic, and the underwater contact angle increased substantially from 54.7 to 155.9°. In addition, compared with LDEA, HLDEA exhibited excellent salt tolerance and enhanced oil recovery performance (the oil recovery was improved by 19.24% at 2.6×10^4 mg/L salinity). Based on nanomechanical experimental results, HLDEA was efficiently adsorbed on the core surfaces and regulated microwetting. Moreover, HLDEA effectively reduced the adhesion force between the alkane chains and the core surface, which facilitated residual oil stripping and oil displacement. This new anionic−nonionic surfactant affording great oil−solid interface wetting control has practical significance for the efficient development of residual oil.

1. INTRODUCTION

Petroleum is an indispensable energy source and an important industrial raw material for maintaining production and life, and it meets approximately half of the total energy demand.[1,2] With the continuous acceleration of global industrialization, the demand for oil resources from countries and individuals has grown rapidly. However, crude oil extracted by conventional means is far from satisfying the requirements for productivity, which increases the gap between crude oil output and refined oil consumption.[3,4] Most of the oil fields in the later stages of water flooding development have entered the high water cut stage, so the residual oil is dispersed and exists in the form of difficult-to-exploit oil droplets, oil films, and blind end oil.[5,6] Overcoming these difficulties to enhance oil recovery is the focus of research on tertiary oil recovery.

Surfactants exhibit low interfacial tension and wetting control, which cause oil droplets to coalesce, form oil belts, and migrate after deformation to produce residual oil.[7−9] Studies have shown that achieving a low interfacial tension effectively increases the number of capillaries and reduces residual oil saturation.[10] However, due to the dominant force between the residual oil and the rock surfaces, it is difficult to realize efficient recovery of oil-film residual oil with low interfacial tension. The wettability of the reservoir rock surface is an important parameter used to characterize interfacial properties, and it affects the peeling efficiencies of oil films adhered to surfaces.[11,12] The long-term contact between the reservoir rock and the crude oil causes the colloidal asphaltene molecules with aromatic rings and alkyl side chains to stack and become entangled due to intermolecular forces, thus forming a solid adsorption layer and making the surface strongly lipophilic.[13,14] The adhesive force between the oil−wet surface and the oil-film residual oil is extremely strong, which makes it difficult to peel off the oil film. Changing the surface wettability to construct a hydrophilic surface would weaken the interaction between the two and enable oil film peeling.[12,15]

Wetting control chemical agents for reservoirs are realized by constructing new hydrophilic surfaces to replace the original lipophilic surfaces. The main mechanism is adsorption, including ion-pairing adsorption, hydrogen adsorption, and

Received: May 3, 2023
Accepted: May 23, 2023
Published: May 31, 2023

Table 1. Formation Water Composition

ion	Na^+	Ca^{2+}	Mg^{2+}	Cl^-	SO_4^{2-}	CO_3^{2-}	T.D.S
concentration (ppm)	7931	1056	720	15,522	353	418	26,000
standard deviation	12	2	2	22	4	3	47

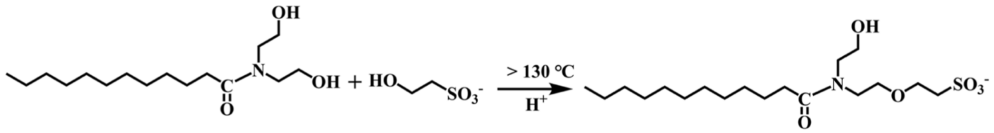

Figure 1. Synthetic route to HLDEA.

hydrophobic adsorption.[16,17] Ion-pairing wetting control agents construct local hydrophilic active sites through electrostatic attraction between the positively charged surfactant molecules and negatively charged formation rock surfaces to modify the surface hydrophilicity.[18,19] However, this wetting modification is not selective, and the adsorption losses are high. The hydrogen adsorption wetting control agent gradually covers the lipophilic surface to form a new hydrophilic surface by forming hydrogen bonds between the molecules and the polar components on the lipophilic rock surface.[20,21] Hydrophobic wetting regulators, due to their strong lipophilicities, rely on hydrophobic interaction forces with the surface lipophilic components to expose hydrophilic groups and construct new hydrophilic surfaces.[22,23] When wetting regulator molecules achieve wetting regulation primarily through hydrophobic forces, they act selectively on lipophilic surfaces, which results in efficient reagent utilization.[24,25] Achieving hydrophilic modifications of rock surfaces through surfactant design and screening is the key to improving residual oil recovery.

Nonionic surfactants exhibit high interfacial activities, which provide surface wetting modifications through hydrophobic interactions and hydrogen adsorption. However, the poor polarity of the hydrophilic end limits the solubility, and the surface is weakly lipophilic or neutral after modification.[26,27] To ensure the formation of environmentally adaptable surfactants, the key is to build highly hydrophilic surfaces through the synergistic effects of hydrophobic and hydrogen bond adsorption to improve residual oil recovery with nonionic surfactants.

In this paper, a novel anionic−nonionic surfactant, sodium laurate ethanolamide sulfonate (HLDEA), which contains one hydrophobic tail chain and hydrophilic heads containing hydroxyl groups and sulfonic acid groups, was prepared via a one-step reaction. The solubility, interfacial tension reduction, wettability reversal, and oil displacement performance of HLDEA were investigated by varying the formation temperature and salt environment. The results showed that HLDEA altered the wettabilities of rock surfaces from strongly lipophilic to strongly hydrophilic, which significantly improved oil recovery. The micromechanism for wetting regulation from the perspective of nanomechanics was revealed via the atomic force microscopy (AFM) technique, which provided theoretical guidance for further optimization of the surfactant molecular design.

2. EXPERIMENTAL SECTION

2.1. Chemicals and Materials. Laurate diethanolamide (LDEA) with a purity above 99% was purchased from Jiangsu Hai'an Petrochemical Plant. Sodium hydroxyethyl sulfonate (SHES) was purchased from Aladdin Chemical Reagent Co., Ltd. (Shanghai, China). Concentrated sulfuric acid, dimethyl sulfoxide, sodium hydroxide, isopropyl alcohol, cyclohexanone, benzalkonium chloride (BAC), methylene blue, acid sodium sulfate, trichloromethane, sodium chloride (NaCl), calcium chloride, magnesium chloride hexahydrate, and other inorganic salts were purchased from Sinopharm Chemical Reagent Co., Ltd. The simulated formation water was a $CaCl_2$ water type and was based on the ionic components shown in Table 1. Crude oil was supplied by the Shengli Oilfield and configured with kerosene to give a mass ratio of 7:3 to form simulated oil. Cores were purchased from Beijing Anmei Petroleum Scientific Research Instrument Co., Ltd. Ultra-pure water was prepared with a reverse osmosis unit (UPT-II-5T, Chengdu ULUPURE Ultrapure Technology Co., Ltd.).

2.2. Synthesis and Characterization. The synthetic route to the anionic−nonionic surfactant (HLDEA) is shown in Figure 1. LDEA, SHES, dimethyl sulfoxide (solvent), and concentrated sulfuric acid (catalyst) were put into three flasks in this order according to certain proportions and heated to 140−170 °C for 18−22 h. The effects of the molar reactant ratios, reaction times, reaction temperatures, and catalyst dosages on the yield were investigated. Sodium hydroxide was added to adjust the pH of the system to neutral. Dimethyl sulfoxide and a small amount of water were removed by rotary evaporation, and the unreacted SHES and the neutralization product sodium sulfate were removed by filtration and then washed with isopropanol until the washing solutions were colorless. A deep brown viscous liquid was obtained by rotary evaporation and the removal of isopropanol. After dissolving the viscous liquid in ultrapure water, cyclohexanone was added to extract the unreacted LDEA, which was dehydrated by rotary evaporation to obtain a light-yellow liquid product.[28,29]

The product content was determined by the *Determination of anionic-active matter content-Direct two-phase titration procedure (GB/T 5173-2018)*. A 0.30 g sample was accurately weighed with an electronic balance and dissolved in 20.00 mL of deionized (DI) water. Then, 5.00 mL of acidic sodium sulfate and 30.00 mL of chloroform were added to a conical flask. After stirring, approximately 1.50 mL of methylene blue indicator was added. A calibrated 0.05 mol/L BAC standard solution was titrated until the lower blue layer disappeared and became light yellow at the titration end point. The amount of BAC standard solution was recorded, and the yield of HLDEA was calculated according to eq 1, where X is the yield of the reaction (%), c is the molar concentration of the BAC standard solution (mol/L), V is the volume of the BAC standard solution consumed by the titration sample (mL), M is the molar mass of the HLDEA product molecule (g/mol), m_1 is the total mass of the product mixture (g), m_2 is the mass of the

https://doi.org/10.1021/acsomega.3c03054
ACS Omega 2023, 8, 21341−21350

sample (g), and m_3 is the theoretical product mass after the completion of the first reaction (g).

$$X\% = \frac{cVMm_1}{1000m_2m_3} \times 100\% \quad (1)$$

The structure of HLDEA was characterized by Fourier transform infrared spectroscopy (FTIR, FTLA2000-104, ABB Bomen Corporation) and ^{1}H nuclear magnetic resonance (NMR, Bruker Avance 300), with deuterated dimethyl sulfoxide (DMSO) as the solvent. FTIR test samples were prepared by the potassium bromide (KBr) pellet method.

2.3. Stability Evaluation. The solubilities of LDEA and modified HLDEA in NaCl and calcium ion solutions were evaluated according to the *Surface Active Agents-Determination of Stability in Hard Water (GB/T 7381-2010)*. Stock solutions of LDEA and HLDEA with mass concentrations of 0.3 wt % were prepared with ultrapure water. Different masses of NaCl/calcium chloride were added to the mother liquor, and a surfactant solution with a mass concentration of 0.3 wt % was prepared with different salinities. The solution was allowed to stand at 25 ± 2 °C for 6 h. The appearance of the solution was observed and identified as clear, milky, or turbid and with a small amount of precipitation or a great deal of precipitation.

Cores were polished and sieved to separate the sand particles with particle sizes of approximately 70 mesh. The sand particles were sieved again after ultrasonic cleaning and drying to complete the pretreatment of the sand particles. The resin and asphaltene components in the crude oil were extracted via the *Test method for separation of asphalt into four fractions* (*NB/SH/T 0509-2010*) and prepared into a colloidal asphaltene/toluene solution with a mass fraction of 0.1 wt %. The pretreated gravel was immersed in the colloidal asphaltene/toluene solution, sealed, and then aged at 75 °C for 48 h. The treated sand and the untreated sand were placed in LDEA and HLDEA solutions with different concentrations and a mass ratio of 1:20 and oscillated at 75 °C for 24 h. The zeta potential of the sand surface was measured after the surfactant treatment with an Omni Zeta potential instrument (NanoBrook Omni, Brookhaven Instruments, U.S.A).

2.4. Surface Tension and Interfacial Tension Measurements. The surface tensions of LDEA and HLDEA in solutions prepared with ultrapure water and different concentrations (from 1×10^{-6} to 5×10^{-1} wt %) were measured by an interfacial rheometer (Tracker-S) at 25 °C. The surface tension was recorded to determine the critical micelle concentrations (CMCs) of LDEA and HLDEA. LDEA and HLDEA solutions with different concentrations (from 0.05 to 0.5 wt %) were prepared with simulated formation water. An interfacial tension meter (TX-500C, KRÜSS) was employed to test the oil/water interfacial tension between oil and the LDEA/HLDEA solutions at 75 °C and 6000 rpm.

2.5. Contact Angle Measurements. The experimental cores were cut into approximately 3 mm thick discs and polished with sandpaper. The surfaces were immersed in ultrapure water for ultrasonic washing for 2 h and then dried at 90 °C to obtain flat and clean core surfaces. The cores were subjected to lipophilic treatment (as mentioned above), and the colloidal asphaltenes that were not firmly adhered were washed away with *n*-heptane solution. After aging at 75 °C for 72 h, an oil−wet surface with colloidal asphaltene deposition was obtained. LDEA and HLDEA solutions with different concentrations (from 0.05 to 0.5 wt %) were prepared with the simulated formation water. The lipophilic sandstone surface was slowly immersed in the solution, sealed, and treated at 75 °C for 24 h. The underwater oil contact angles of the oleophilic cores treated with the simulated formation water and LDEA and HLDEA solutions were measured with a contact angle meter (JC2000D).

2.6. Oil Displacement Evaluation. The sandstone core parameters used in this experiment are shown in Table 2. The

Table 2. Core Parameters for Oil Displacement

core	length (mm)	diameter (mm)	pore volume (cm^3)	permeability (10^{-3} μm^2)	oil saturation (%)
number	49.64	25.15	5.71	51.48	94.06
standard deviation	1.11	0.03	0.23	0.66	0.50

physical simulation core flooding device is shown in Figure 2. The simulated oil was introduced into the cores by vacuum saturation, which were then aged at 75 °C for 7 days. The displacement experiments were conducted at 75 °C with a flow rate of 0.3 mL/min. The displacement fluid with a mass concentration of 0.3 wt % and 3 times the pore volume (PV) was completely injected until the water content in the produced liquid exceeded 98%. The resulting liquid was collected, and the recovery factor was calculated.

2.7. Wetting Regulation Mechanism. The adsorption morphologies of the surfactants were observed by AFM (Multimode 8) in tapping mode. The oleophilic core surface was obtained as described earlier. The samples were prepared by immersing the oleophilic cores into 0.3 wt % LDEA and 0.1 wt % HLDEA (near the CMC) at 75 °C for 10 min and dried by nitrogen flow. The morphologies were characterized for comparison.

A gold-plated probe (NPG-10) was functionalized with a 5 wt % *N*-dodecanethiol solution in ethanol via Au−S bonding to fabricate the dodecane-functionalized hydrophobic probe.[30] Straight-chain alkanes were used to simulate the hydrophobic components of crude oil. Successful preparation of the hydrophobic probe was confirmed with scanning electron microscopy (SEM, JSM-7610F) and energy-dispersive spectrometry (EDS, S-4800 Hitachi), as shown in Figure S1. In the DI water environment, the adhesive forces between the hydrophobic probe and oleophilic cores treated with 0.3 wt % LDEA and 0.1 wt % HLDEA (near the CMC) were measured in force-volume mode.

3. RESULTS AND DISCUSSION

3.1. Characterization of the Synthesized Surfactant. The effects of the molar ratio of LDEA to SHES, reaction temperature, reaction time, and catalyst dosage on the yield for dehydration to ether were investigated, and the results are shown in Figure S2. Overall, the optimum reaction conditions were *n* (LDEA)/*n* (SHES) = 1:2.0, a reaction temperature of 160 °C, a reaction time of 20 h, and a catalyst dosage of 3%. The highest yield of HLDEA (89.33%) was achieved with these reaction conditions.

The FTIR spectra of LDEA and HLDEA are shown in Figure 3. For both compounds, the O−H, C−H, and C−N stretching vibrations were indicated by peaks near 3360, 2920, and 1040 cm^{-1}. In addition to these peaks, the S═O stretching vibrational peak at 1215.97 cm^{-1} and the C−O−C bond stretching vibrational peak at 1168.25 cm^{-1} appeared in

https://doi.org/10.1021/acsomega.3c03054
ACS Omega 2023, 8, 21341−21350

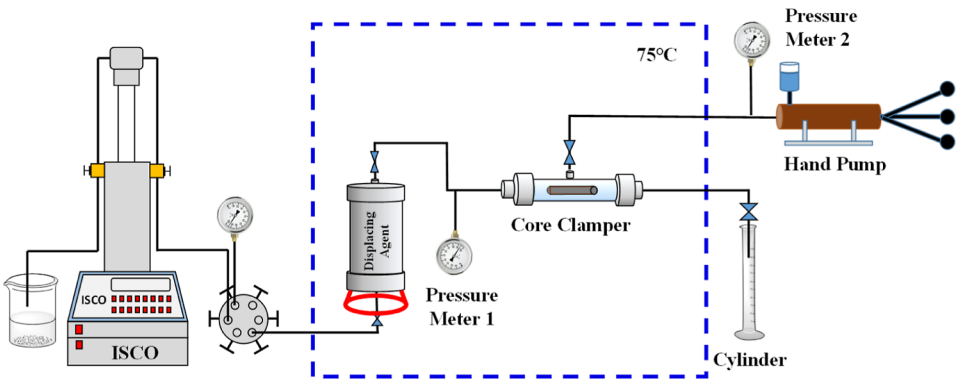

Figure 2. Apparatus for the physical simulation experiments.

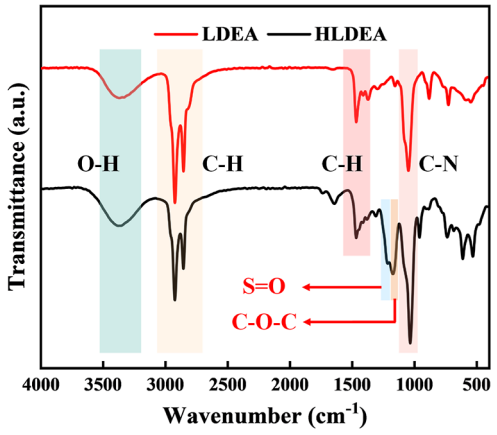

Figure 3. FTIR spectra of LDEA and HLDEA.

the spectrum of HLDEA. The vibrational peaks for C−O−C bonds and S═O bonds indicated the generated ether bonds and the introduced sulfonic acid groups. The presence of these two peaks proved the successful reaction and grafting of the sulfonic acid groups to the LDEA molecules.

The ^{1}H NMR spectrum of HLDEA is shown in Figure 4. The characteristic signal at δ = 4.64 ppm was attributed to the

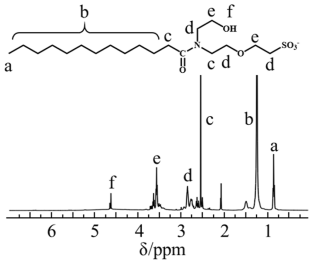

Figure 4. ^{1}H NMR spectrum of HLDEA.

hydroxyl (−OH) proton. The integrated peak area was 0.84, indicating only one hydroxyl group in the molecule. The multiplets at δ = 2.58−2.96 ppm and δ = 3.51−3.72 ppm were for methylene protons between the amide group and the hydroxyl and ether groups, respectively. The singlet at δ = 2.55 ppm was for the two methylene groups near the amide group. The aliphatic methylene $(-CH_2-)_n$ protons showed a strong peak at δ = 1.25 ppm, and the terminal methyl $(-CH_3)$ protons were indicated by the presence of a peak at δ = 0.86 ppm. The ^{1}H NMR spectrum confirmed the presence of the expected functional groups in the synthesized surfactant.

3.2. Stability. To reduce the sedimentation loss of the oil displacement agent system and maintain the effective concentration, the solubility of the surfactant in the formation environment was evaluated. Salt ions have the greatest influence on the solubilities of surfactants in the formation environment, so the effects of NaCl and calcium ions on the solubility were evaluated experimentally. The physical diagrams for LDEA and HLDEA are shown in Figure 5a,c for different salinities. When the concentration of NaCl was more than 2×10^4 mg/L, LDEA changed from turbid to milky, indicating that the stability of the solution itself was destroyed. However, the HLDEA solution maintained a clear and transparent stable state when the concentration of NaCl was lower than 27×10^4 mg/L. Only when the concentration was 30×10^4 mg/L did the solution begin to turn milky. With the increased salinity, there was no floccule formation or precipitation during the whole process. The stability of HLDEA in the NaCl solution was significantly higher than that of LDEA, and the upper limit for NaCl tolerance was higher than 27×10^4 mg/L.

Figure 5b also shows that the solubility of LDEA in a calcium-containing solution was very poor, and the addition of a small amount of calcium ions (600 mg/L) to an LDEA solution caused the solution to become turbid. After grafting the sulfonic acid groups, the molecular hydrophilicity and intermolecular electrostatic repulsion were enhanced to improve the stability of HLDEA in the calcium-containing solution.[31] When the calcium ion concentration was more than 2.7×10^4 mg/L, the HLDEA solution began to appear milky (Figure 5d). HLDEA had a high upper limit for salt tolerance and could be applied to most reservoirs.

Surfactant molecules adsorbed on the surface of the sand to change the stability of the sand itself. Surfactants containing anionic groups increased the surface charge density, thereby changing the surface potential of the sand particles. The zeta potential data for the water−wet sands and oil−wet sands after the LDEA and HLDEA treatments are shown in Figure 6. Figure 6a shows that the initial zeta potential was negative due to the inherent negative charge on the surfaces of the sand particles. With increasing LDEA concentration, the surface zeta potential decreased gradually but slightly. The surface zeta potential at a 0.5 wt % concentration was −6.93 mV, which was still unstable. As the concentration of HLDEA increased, the zeta potential of the modified sand surface decreased faster than that of LDEA. The zeta potential of the 0.4 wt %

https://doi.org/10.1021/acsomega.3c03054
ACS Omega 2023, 8, 21341−21350

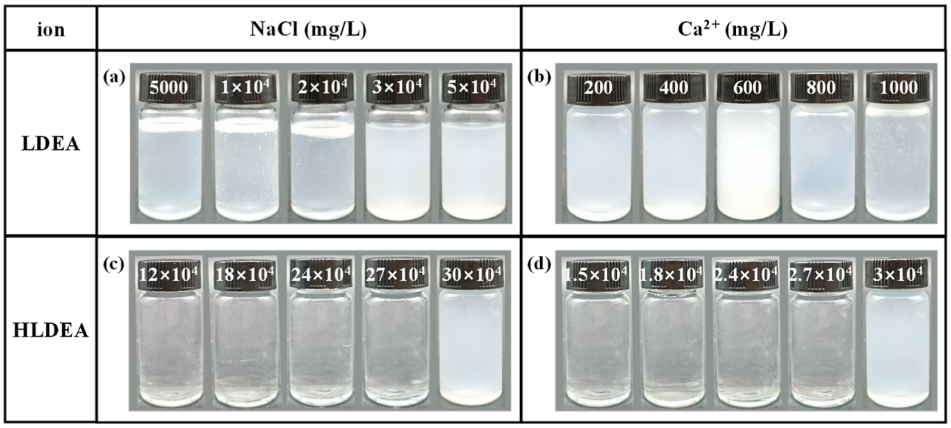

Figure 5. Effects of NaCl (a,c) and Ca^{2+} (b,d) on the solubilities of LDEA and HLDEA.

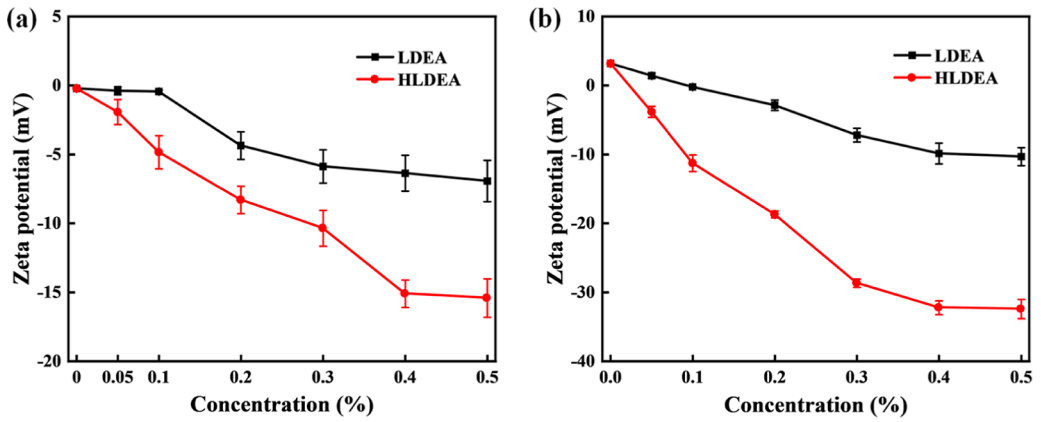

Figure 6. Surface potentials of the water−wet sand surface (a) and oil−wet sand surface (b).

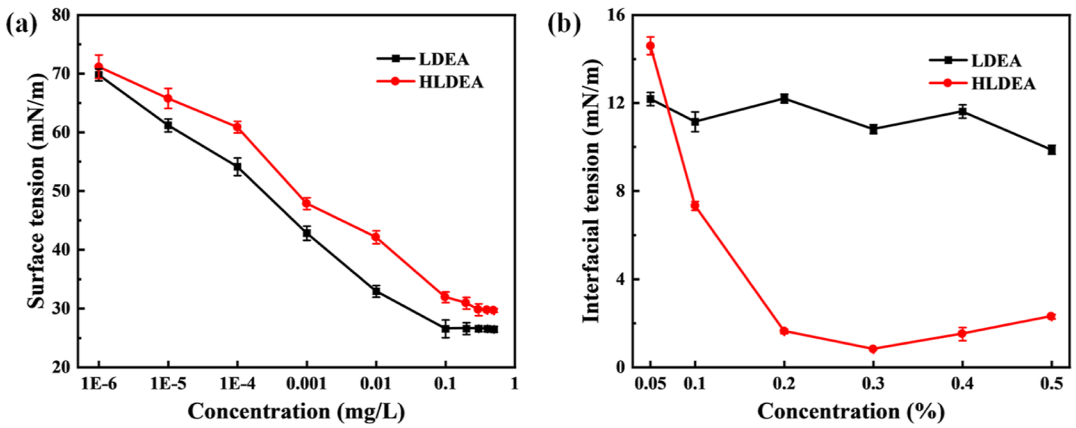

Figure 7. Surface tension (a) and interfacial tension (b) curves for HLDEA and LDEA with different concentrations.

HLDEA-modified surface was −15.09 mV, which was significantly higher than that of LDEA.

The zeta potential data for the oil−wet sands are shown in Figure 6b. The adsorption of LDEA on the surface of oil−wet sand produced little effect on its surface potential. The surface zeta potential decreased to −10.32 mV at a 0.5 wt % concentration and was still in a relatively unstable state. With increasing HLDEA concentration, the surface zeta potential decreased to −32.22 mV, which increased the negative charge on the sand surface. HLDEA was adsorbed on the sand surface through the hydrophobic tail to expose the hydrophilic sulfonic acid, which improved the surface negative charge density and the stability of the sands in solution.[32]

3.3. Surface Tension and Interfacial Tension. Figure 7a shows that the surface tensions generated with the two surfactants decreased rapidly and then basically remained invariant with increasing concentration. The surfactant molecules in water first floated on the surface due to surface tension. After the surface was covered with the surfactant molecules, the molecules began to form micelles in the solution, and the corresponding concentration was defined as the CMC.[33] The CMCs of HLDEA and LDEA were found to be 0.3 and 0.1 wt %, respectively. Due to electrostatic repulsion

https://doi.org/10.1021/acsomega.3c03054
ACS Omega 2023, 8, 21341−21350

between the hydrophilic sulfonic acids, HLDEA caused the molecules to reach saturation on the surface faster and reduced the CMC.

The ability of the surfactant to reduce the oil−water interfacial tension strongly influenced the residual oil utilization capacity. The oil−water interfacial tensions for LDEA and HLDEA at 75 °C are shown in Figure 7b. The oil−water interfacial tension of LDEA varied in the range of 9−12 mN/m, and the concentration had little effect. Due to the strong lipophilicity of LDEA, fewer surfactant molecules in the solution were distributed at the oil−water interface and tended to enter the oil phase, making it difficult to reduce the interfacial tension further. With increasing HLDEA concentration, the oil−water interfacial tension decreased first and then increased. The lowest oil−water interfacial tension occurred at 0.3 wt % and was 0.82 mN/m. The enhanced hydrophilicity of the modified HLDEA increased the number of surfactant molecules at the oil−water interface relative to the number seen before modification. The ability of HLDEA to reduce the oil−water interfacial tension was significantly greater than that of LDEA.[34]

3.4. Contact Angle. In the exploitation of residual oil via water injection, changing the surface wettability effectively strips the surface oil films.[35] The abilities of LDEA and HLDEA to change the wettability were evaluated by measuring the underwater oil contact angles of the gum asphaltene deposited on the core surfaces before and after surfactant modification. The experimental results for changing the underwater oil contact angle on the lipophilic core surface with different concentrations of LDEA and HLDEA are shown in Figure 8. After the oleophilic treatment, the underwater oil

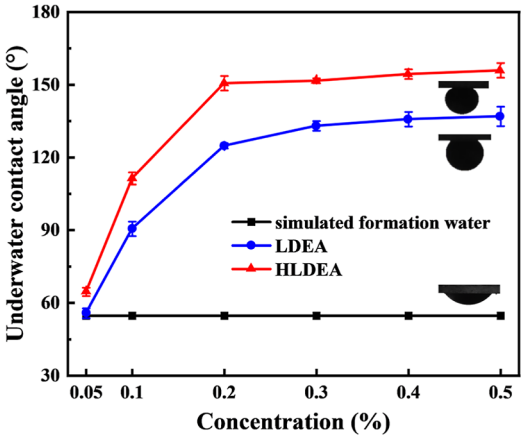

Figure 8. Underwater oil contact angles on the oil−wet core surfaces vary with the concentrations of LDEA and HLDEA.

contact angle on the core was 54.7°, indicating that the surface had been converted to an oil−wet state. When the concentration was higher than 0.05 wt %, the surfaces modified by LDEA and HLDEA gradually transitioned toward water wetness. As the concentration was increased to 0.5 wt %, the underwater oil contact angle of the LDEA-modified surface was 136.9° and that of the HLDEA-modified surface increased to 155.9°. The enhanced solubility of the modified HLDEA in solution made the activity higher than that of the LDEA solution at the same concentration. There were more surfactant molecules on the unit oil−wet surface, which enhanced the wetting control performance. In addition, HLDEA with the strongly hydrophilic sulfonic acid groups formed a hydration layer outside the hydrophilic adsorption layer constructed on the lipophilic surface, which made the modified surface more hydrophilic.[36]

3.5. Oil Displacement. The experimental results described above showed that HLDEA with a concentration of 0.3 wt % exhibited superior performance and achieved a low interfacial tension with oil and regulated interfacial wettability. To further evaluate its practical oil displacement performance, a dynamic core displacement experiment was carried out, and the results are shown in Figure 9. As the injection fluids gradually entered

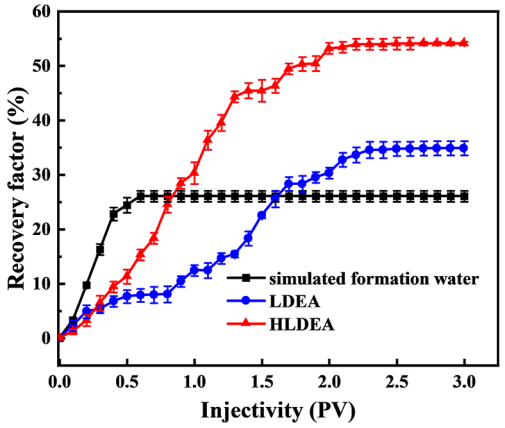

Figure 9. Oil recovery rates for simulated formation water, LDEA, and HLDEA.

the cores, the water flooding recovery rate no longer increased at 0.7 PV. When the water content in the resulting liquid exceeded 98%, the water flooding and 0.3 wt % LDEA recovery factors were calculated as 26.06 and 34.89%, respectively. For 0.3 wt % HLDEA, a recovery factor of 54.13% was attained, which constituted an ∼19.24% increase in oil recovery compared with that of 0.3 wt % LDEA. The improved oil recovery was attributed to the low interfacial tension as well as the wettability reversal caused by the HLDEA. The oil droplets were stripped off by the oil−solid interface effect and detached from the surface. Due to the low interfacial tension, the stripping oil droplets were deformed to overcome the Jamin effect and migrated out of the pores.[37]

3.6. Mechanism of Interface Wetting Regulation. AFM was used to elucidate the mechanism for interface wetting regulation.[38,39] For anionic surfactants, their ability to modify rock surface wettability is closely related to the adsorption capability.[40,41] Therefore, the surface topographies and mean roughness values of the oleophilic cores were characterized after the LDEA and HLDEA treatments. Figure 10 shows three-dimensional (3D) and two-dimensional (2D) microtopography images and surface profiles based on the chosen paths of the different samples. The adsorption layer formed by surfactant molecules on the lipophilic surface was granular with a certain interval and was evenly distributed independently. Figure 10a shows that the adsorption layer of LDEA on the oil−wet core was approximately 14.8 nm thick and had a mean roughness of 4.6 nm. In contrast, the adsorption layer of the oil−wet core treated with HLDEA (Figure 10b) was approximately 21.3 nm thick. Many clusters and spherical particles were observed on the HLDEA layer, which accounted for the increased surface roughness (6.9 nm).

https://doi.org/10.1021/acsomega.3c03054
ACS Omega 2023, 8, 21341−21350

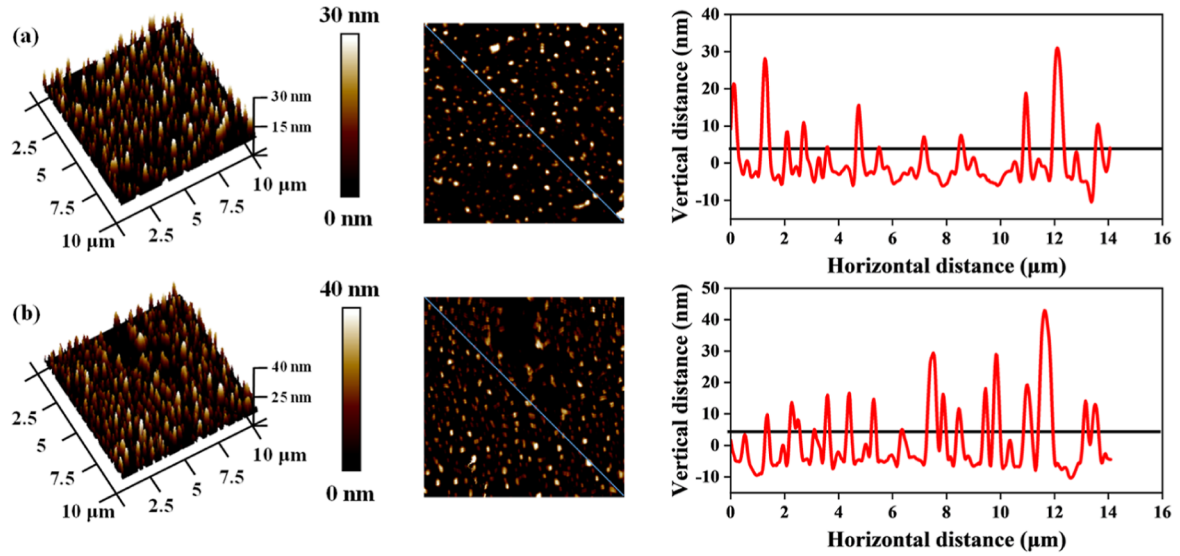

Figure 10. AFM height images of the oleophilic cores treated with LDEA (a) and HLDEA (b).

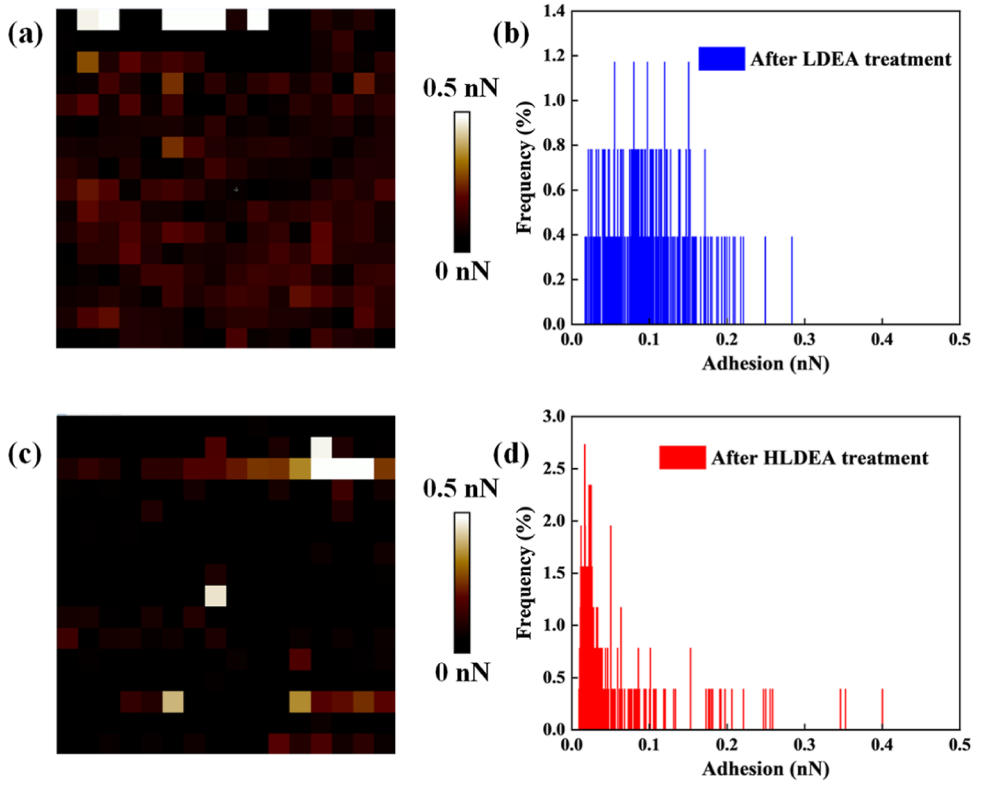

Figure 11. Diagrams and frequency histograms for the adhesion forces between alkane and the core: (a,b) LDEA-treated core and (c,d) HLDEA-treated core.

Based on the AFM results, HLDEA showed a higher adsorption capacity which improved the surface coverage.

AFM was used to study the interactions between the hydrophobic surface and alkanes after the adsorption of LDEA and HLDEA to clarify the mechanism for enhancement. According to the extended DLVO theory, the adhesion forces of colloidal particles include the van der Waals force (vdW), electric double-layer interactions (EDLs), and possible hydrophilic/hydrophobic forces.[42,43] In this experiment, the vdW and the EDL measured before and after the adsorption of LDEA and HLDEA did not contribute to changes in the resultant forces, so the change in the adhesion force comprised the hydrophilic/hydrophobic force.[44] The adhesion force (Figure 11a,c) and frequency distribution histograms (Figure 11b,d) are provided in Figure 11. The colors in the adhesion force diagrams from light to dark indicated that the hydrophobic force decreased and the hydrophilicity increased gradually. It was obvious that the color of the lipophilic core became darker after the HLDEA treatment. Notably, the colors in the adhesion force diagrams in Figure 11a,c were not uniform, which may have been caused by an uneven mineral distribution. In the corresponding force frequency distribution

https://doi.org/10.1021/acsomega.3c03054
ACS Omega 2023, 8, 21341−21350

histogram, the values of the average adhesion forces after the LDEA and HLDEA treatments were 0.0837 and 0.0191 nN, respectively. In contrast to the LDEA treatment, the adhesion force after the HLDEA treatment was significantly lower, and the hydrophilicity was considerably higher. Moreover, the lipophilic surface was more homogeneous based on the obvious narrowing of the distribution range for HLDEA adhesion in the force frequency histogram. The reduced adhesion and wettability alterations functioned simultaneously to strip the oil droplets.

4. CONCLUSIONS

In this paper, a novel HLDEA surfactant designed for residual oil displacement was successfully synthesized by a Williamson etherification reaction of LDEA and SHES. The experimental results showed that the introduction of the sulfonic acid groups greatly increased the salt tolerance and the absolute value of the zeta potential on the surfaces of the sand particles. Compared with LDEA, HLDEA was adsorbed at the oil−water interface and significantly reduced the oil−water interfacial tension. In addition, HLDEA exposed the sulfonate hydrophilic head groups to construct a hydrophilic surface from the hydrophobic force between the long-chain alkanes and the surface lipophilic components, which greatly increased the underwater contact angle from 54.7 to 155.9°. Recovery rates of up to 75% were attained with 0.3 wt % HLDEA core flooding. HLDEA exhibited excellent oil displacement performance as well as wetting regulation performance, and it demonstrated considerable potential for use in efficient oilfield development.

■ ASSOCIATED CONTENT

Supporting Information

The Supporting Information is available free of charge at https://pubs.acs.org/doi/10.1021/acsomega.3c03054.

SEM and EDS images of NPG-10 probe functionalized with 1-dodecanethiol and effects of molar ratio of LDEA to SHES, reaction temperature, reaction time, and catalyst dosage (PDF)

■ AUTHOR INFORMATION

Corresponding Author

Lin Li − *Shandong Key Laboratory of Oilfield Chemistry, Department of Petroleum Engineering, China University of Petroleum (East China), Qingdao 266580, China; Key Laboratory of Unconventional Oil & Gas Development (China University of Petroleum (East China)), Ministry of Education, Qingdao 266580, China;* orcid.org/0000-0001-5003-3634; Email: lilin@upc.edu.cn

Authors

Yue Sun − *Shandong Key Laboratory of Oilfield Chemistry, Department of Petroleum Engineering, China University of Petroleum (East China), Qingdao 266580, China; Key Laboratory of Unconventional Oil & Gas Development (China University of Petroleum (East China)), Ministry of Education, Qingdao 266580, China*

Xiao Jin − *Shandong Key Laboratory of Oilfield Chemistry, Department of Petroleum Engineering, China University of Petroleum (East China), Qingdao 266580, China; Key Laboratory of Unconventional Oil & Gas Development (China University of Petroleum (East China)), Ministry of Education, Qingdao 266580, China*

Zizhao Wang − *Shandong Key Laboratory of Oilfield Chemistry, Department of Petroleum Engineering, China University of Petroleum (East China), Qingdao 266580, China; Key Laboratory of Unconventional Oil & Gas Development (China University of Petroleum (East China)), Ministry of Education, Qingdao 266580, China*

Yunbo Dong − *Shandong Key Laboratory of Oilfield Chemistry, Department of Petroleum Engineering, China University of Petroleum (East China), Qingdao 266580, China; Key Laboratory of Unconventional Oil & Gas Development (China University of Petroleum (East China)), Ministry of Education, Qingdao 266580, China*

Caili Dai − *Shandong Key Laboratory of Oilfield Chemistry, Department of Petroleum Engineering, China University of Petroleum (East China), Qingdao 266580, China; Key Laboratory of Unconventional Oil & Gas Development (China University of Petroleum (East China)), Ministry of Education, Qingdao 266580, China;* orcid.org/0000-0002-7477-8865

Mingwei Zhao − *Shandong Key Laboratory of Oilfield Chemistry, Department of Petroleum Engineering, China University of Petroleum (East China), Qingdao 266580, China; Key Laboratory of Unconventional Oil & Gas Development (China University of Petroleum (East China)), Ministry of Education, Qingdao 266580, China;* orcid.org/0000-0002-9671-8206

Yining Wu − *Shandong Key Laboratory of Oilfield Chemistry, Department of Petroleum Engineering, China University of Petroleum (East China), Qingdao 266580, China; Key Laboratory of Unconventional Oil & Gas Development (China University of Petroleum (East China)), Ministry of Education, Qingdao 266580, China;* orcid.org/0000-0001-6884-4865

Complete contact information is available at: https://pubs.acs.org/10.1021/acsomega.3c03054

Author Contributions

Credit author statement. Lin Li: writing-original draft, writing-review and editing. **Yue Sun**: writing-original draft, investigation. **Xiao Jin**: data curation. **Zizhao Wang**: formal analysis. **Yunbo Dong**: methodology. **Caili Dai**: resources, supervision, writing-review and editing. **Mingwei Zhao**: supervision. **Yining Wu**: validation.

Notes

The authors declare no competing financial interest.

■ ACKNOWLEDGMENTS

This study is financially supported by the National Key Research and Development Program of China (no. 2019YFA0708700) and the National Natural Science Foundation of China (52174054).

■ REFERENCES

(1) Alzahid, Y. A.; Mostaghimi, P.; Walsh, S. D. C.; Armstrong, R. T. Flow regimes during surfactant flooding: The influence of phase behaviour. *Fuel* **2019**, *236*, 851−860.

(2) Alvarado, V.; Manrique, E. Enhanced oil recovery: an update review. *Energies* **2010**, *3*, 1529−1575.

(3) Farrokhi, F. Global sourcing in oil markets. *J. Int. Econ.* **2020**, *125*, 103323.

(4) Sun, Z.; Cai, X.; Huang, W.-C. The impact of oil price fluctuations on consumption, output, and investment in china's industrial sectors. *Energies* **2022**, *15*, 3411.
(5) Zhao, H.; Yang, H. B.; Kang, X.; Jiang, H. Z.; Li, M. L.; Kang, W. L.; Sarsenbekuly, B. Study on the types and formation mechanisms of residual oil after two surfactant imbibition. *J. Pet. Sci. Eng.* **2020**, *195*, 107904.
(6) Fan, J.; Liu, L.; Ni, S.; Zhao, J. Displacement mechanisms of residual oil film in 2D microchannels. *ACS Omega* **2021**, *6*, 4155−4160.
(7) Li, Q.; Ding, M.; Zhang, X.; Wu, H.; Chen, L.; Wang, Y. Adaptability of an in-situ microemulsion surfactant in displacing the high-pour-point oil from low permeability reservoir. *Oilfield Chem.* **2022**, *39*, 474−479.
(8) Chen, J.; Huang, Z.; Liu, D.; Zhang, Y.; Li, H.; Lu, H. Wettability reversal of reservoir rock surface through surfactant stabilized microemulsion. *J. Surfactants Deterg.* **2022**, *25*, 527−536.
(9) Yang, S.; Zhang, C.; Pan, Y.; Yang, E.; Guo, Y. Research advance in the oil-displacement effect of ASP flooding system. *Mo. Chem. Ind.* **2017**, *37*, 28−32.
(10) Dong, M.; Chatzis, I. An experimental investigation of retention of liquids in corners of a square capillary. *J. Colloid Interface Sci.* **2004**, *273*, 306−312.
(11) Li, L.; Wang, Z.; Liu, J.; Chen, J.; Jin, X.; Dai, C. Synthesis and performance evaluation of polyhydroxy benzene sulfonate oil displacement agent based on enhanced interfacial wettability control. *Acta Chim. Sin.* **2022**, *80*, 63−68.
(12) Lin, M.; Hua, Z.; Li, M. Surface wettability control of reservoir rocks by brine. *Petrol. Explor. Dev.* **2018**, *45*, 145−153.
(13) Khormali, A.; Sharifov, A. R.; Torba, D. I. Experimental and modeling study of asphaltene adsorption onto the reservoir rocks. *Pet. Sci. Technol.* **2018**, *36*, 1482−1489.
(14) Wang, S.; Liu, Q.; Tan, X.; Xu, C.; Gray, M. R. Adsorption of asphaltenes on kaolinite as an irreversible process. *Colloids Surf., A* **2016**, *504*, 280−286.
(15) Li, L.; Chen, J.; Xu, X.; Liu, J.; Xu, Z.; Sun, W.; Zhu, Z.; Dai, C. Preparation and performance evaluation of oil-displacing agent with interfacial wettability control. *Oilfield Chem.* **2021**, *38*, 90−94.
(16) Dalvand, A.; Asleshirin, S.; Fallahiyekta, M. Hydrophobic silica nanoparticle and anionic/cationic surfactants interplays tailored interfacial properties for the wettability alteration and EOR applications. *Iran. J. Chem. Chem. Eng. (Int. Engl. Ed.)* **2022**, *41*, 1076−1094.
(17) Shahbazi, E.; Moradzadeh, A.; Khandoozi, S.; Riazi, M. Experimental investigation of the controversial effects of a cationic surfactant with brine on spontaneous imbibition of an asphaltenic crude oil. *J. Mol. Liq.* **2022**, *362*, 119687.
(18) Deng, X.; Kamal, M. S.; Patil, S.; Hussain, S. M. S.; Mahmoud, M.; Al Shehri, D.; Abu-Khamsin, S.; Mohanty, K. Wettability alteration on carbonate rock by the mixture of the gemini surfactant and chelating agent. *Energy Fuels* **2022**, *36*, 13652−13664.
(19) Du, A.; Mao, J.; Wang, D.; Hou, C.; Lin, C.; Yang, X.; Cao, H.; Mao, J. Wettability alteration at a water-wet quartz surface by a novel trimeric surfactant: Experimental and theoretical study. *J. Mol. Liq.* **2022**, *354*, 118771.
(20) He, X.; Zhang, L.-H.; Shen, Q. Quantitatively evaluation of the hydrogen bonding, wettability and sorption behaviors of poly(vinyl alcohol)/tea polyphenols composites. *J. Polym. Res.* **2022**, *29*, 485.
(21) Li, L.; Liu, M.; Lyu, J.; Li, X.; Li, Z.; Lin, M.; Ma, C.; He, M.; Wang, Q.; Yu, H.; et al. Effect of bio-based surfactant on wettability of low-rank coal surface and its mechanism. *Environ. Sci. Pollut. Res.* **2022**, *29*, 39610−39621.
(22) Chen, X.; Liu, J.; Yan, G.; Li, J.; Bai, X. Molecular mechanism of hydrophobic tail chain saturation in nonionic surfactants changing the wettability of anthracite. *J. Mol. Liq.* **2022**, *368*, 120732.
(23) Staniscia, F.; Guzman, H. V.; Kanduc, M. Tuning contact angles of aqueous droplets on hydrophilic and hydrophobic surfaces by surfactants. *J. Phys. Chem. B* **2022**, *126*, 3374−3384.
(24) Xie, L.; Yang, D. L.; Lu, Q. Y.; Zhang, H.; Zeng, H. B. Role of molecular architecture in the modulation of hydrophobic interactions. *Curr. Opin. Colloid Interface Sci.* **2020**, *47*, 58−69.
(25) Yin, X.; Miller, J. D. Wettability of kaolinite basal planes based on surface force measurements using atomic force microscopy. *Miner. Metall. Process.* **2012**, *29*, 13−19.
(26) Souayeh, M.; Al-Maamari, R. S.; Karimi, M.; Aoudia, M. Wettability alteration and oil recovery by surfactant assisted low salinity water in carbonate rock: The impact of nonionic/anionic surfactants. *J. Pet. Sci. Eng.* **2021**, *197*, 108108.
(27) Torabi, F.; Ruiz, M. G.; Mohammadpoor, M.; Wilton, R. R. Wettability modification and its impact on oil recovery. *Energy Sources, Part A* **2015**, *37*, 1300−1307.
(28) Allen, M. C.; Hoffman, A. J.; Liu, T.-w.; Webber, M. S.; Hibbitts, D.; Schwartz, T. J. Highly Selective Cross-Etherification of 5-Hydroxymethylfurfural with Ethanol. *ACS Catal.* **2020**, *10*, 6771−6785.
(29) Da Silva, M. J.; Julio, A. A.; Ferreira, S. O.; Da Silva, R. C.; Chaves, D. M. Tin(II) phosphotungstate heteropoly salt: An efficient solid catalyst to synthesize bioadditives ethers from glycerol. *Fuel* **2019**, *254*, 115607.
(30) Li, L.; Chen, J.; Liu, J.; Xu, Z.; Wu, Y.; Zhao, M.; Zhao, G.; Dai, C. Anionic surfactant based on oil-solid interfacial interaction control for efficient residual oil development. *Colloids Surf., A* **2022**, *648*, 129396.
(31) Wibowo, A. D. K.; Yoshi, L. A.; Handayani, A. S.; Joelianingsih. Synthesis of polymeric surfactant from palm oil methyl ester for enhanced oil recovery application. *Colloid Polym. Sci.* **2021**, *299*, 81−92.
(32) Khaleel, O.; Teklu, T. W.; Alameri, W.; Abass, H.; Kazemi, H. Wettability alteration of carbonate reservoir cores-laboratory evaluation using complementary techniques. *SPE Reservoir Eval. Eng.* **2019**, *22*, 911−922.
(33) Belhaj, A. F.; Elraies, K. A.; Alnarabiji, M. S.; Abdul Kareem, F. A.; Shuhli, J. A.; Mahmood, S. M.; Belhaj, H. Experimental investigation, binary modelling and artificial neural network prediction of surfactant adsorption for enhanced oil recovery application. *Chem. Eng. J.* **2021**, *406*, 127081.
(34) Li, Y. M.; Guo, Y. Y.; Bao, M. T.; Gao, X. L. Investigation of interfacial and structural properties of CTAB at the oil/water interface using dissipative particle dynamics simulations. *J. Colloid Interface Sci.* **2011**, *361*, 573−580.
(35) Zargar, G.; Takassi, M. A.; Moradi, S.; Rostami, A. R.; Jabari, B. Evaluation of a new agent for wettability alteration during enhanced oil recovery. *Iran. J. Chem. Chem. Eng. (Int. Engl. Ed.)* **2020**, *39*, 333−341.
(36) Chen, S.; Han, M.; AlSofi, A. M.; Fahmi, M. M. Experimental evaluation of non-ionic mixed surfactant formulations at high-temperature and high-salinity conditions. *J. Pet. Sci. Eng.* **2022**, *219*, 111084.
(37) Liu, S.; Dou, X. X.; Zeng, Q. D.; Liu, J. L. Critical parameters of the Jamin effect in a capillary tube with a contracted cross section. *J. Pet. Sci. Eng.* **2021**, *196*, 107635.
(38) Hou, B.; Jia, R.; Fu, M.; Wang, Y.; Bai, Y.; Huang, Y. Wettability alteration of an oil-wet sandstone surface by synergistic adsorption/desorption of cationic/nonionic surfactant mixtures. *Energy Fuels* **2018**, *32*, 12462−12468.
(39) Kékicheff, P.; Contal, C. Cationic-surfactant-coated mica surfaces below the critical micellar concentration: 1. patchy structures as revealed by peak force tapping afm mode. *Langmuir* **2019**, *35*, 3087−3107.
(40) Liu, Z.; Zhao, G.; Brewer, M.; Lv, Q.; Sudholter, E. J. R. Comprehensive review on surfactant adsorption on mineral surfaces in chemical enhanced oil recovery. *Adv. Colloid Interface Sci.* **2021**, *294*, 102467.
(41) Li, S.; Torsaeter, O.; Lau, H. C.; Hadia, N. J.; Stubbs, L. P. The impact of nanoparticle adsorption on transport and wettability alteration in water-wet berea sandstone: an experimental study. *Front. Phys.* **2019**, *7*, 74.

https://doi.org/10.1021/acsomega.3c03054
ACS Omega 2023, 8, 21341−21350

(42) Xie, L.; Shi, C.; Wang, J.; Huang, J.; Lu, Q.; Liu, Q.; Zeng, H. Probing the interaction between air bubble and sphalerite mineral surface using atomic force microscope. *Langmuir* **2015**, *31*, 2438−2446.
(43) Liu, J.; Cui, X.; Xie, L.; Huang, J.; Zhang, L.; Liu, J.; Wang, X.; Wang, J.; Zeng, H. Probing effects of molecular-level heterogeneity of surface hydrophobicity on hydrophobic interactions in air/water/solid systems. *J. Colloid Interface Sci.* **2019**, *557*, 438−449.
(44) Hendraningrat, L.; Torsaeter, O. Metal oxide-based nanoparticles: revealing their potential to enhance oil recovery in different wettability systems. *Appl. Nanosci.* **2015**, *5*, 181−199.

https://doi.org/10.1021/acsomega.3c03054
ACS Omega 2023, 8, 21341−21350